Human Molecular Genetics, 2001, Vol. 10, No. 8 865–874

Positional cloning of a novel gene on chromosome 16q causing Bardet–Biedl syndrome (BBS2)

Darryl Y. Nishimura[1], Charles C. Searby[1], Rivka Carmi[2], Khalil Elbedour[2], Lionel Van Maldergem[3], Anne B. Fulton[4], Byron L. Lam[5], Berkley R. Powell[6], Ruth E. Swiderski[1], Kevin E. Bugge[1], Neena B. Haider[7], Anne E. Kwitek-Black[8], Lihua Ying[1], David M. Duhl[9], Susan W. Gorman[9], Elise Heon[10], Alessandro Iannaccone[11], Dominique Bonneau[12], Leslie G. Biesecker[13], Samuel G. Jacobson[14], Edwin M. Stone[15] and Val C. Sheffield[1,+]

[1]Department of Pediatrics and Howard Hughes Medical Institute, University of Iowa, Iowa City, IA 52242, USA, [2]Soroka Medical Center, Ben-Gurion University of the Negev, Beer-Sheva, Israel, [3]Centre de Genetique Humaine, Institute de Pathologie et de Genetique, Loverval, Belgium, [4]Department of Ophthalmology, Children's Hospital and Harvard Medical School, Boston, MA, USA, [5]Bascom Palmer Eye Institute, Miami, FL 33136, USA, [6]Valley Children's Hospital, Madera, CA 93638, USA, [7]The Jackson Laboratory, Bar Harbor, ME 04609, USA, [8]Medical College of Wisconsin, Milwaukee, WI 53226, USA, [9]Chiron Corporation, Emeryville, CA 94608, USA, [10]Vision Science Research Program, Toronto Western Research Institute, Toronto, Canada, [11]Department of Ophthalmology, University of Tennessee Health Science Center, Memphis, TN 38103, USA, [12]Department of Medical Genetics, University of Poitiers, Poitiers, France, [13]National Human Genome Research Institute, The National Institutes of Health, Bethesda, MD 20892, USA, [14]Scheie Eye Institute, Philadelphia, PA 19104, USA, [15]Department of Ophthalmology, University of Iowa, Iowa City, IA 52242, USA

Received 29 December 2000; Revised and Accepted 5 February 2001 DDBJ/EMBL/GenBank accession nos AF342736–AF342739

Bardet–Biedl syndrome (BBS) is a genetically heterogeneous autosomal recessive disorder with the primary clinical features of obesity, pigmented retinopathy, polydactyly, hypogenitalism, mental retardation and renal anomalies. Associated features of the disorder include diabetes mellitus, hypertension and congenital heart disease. There are six known BBS loci, mapping to chromosomes 2, 3, 11, 15, 16 and 20. The BBS2 locus was initially mapped to an 18 cM interval on chromosome 16q21 with a large inbred Bedouin kindred. Further analysis of the Bedouin population allowed for the fine mapping of this locus to a 2 cM region distal to marker *D16S408*. Physical mapping and sequence analysis of this region resulted in the identification of a number of known genes and expressed sequence tag clusters. Mutation screening of a novel gene (*BBS2*) with a wide pattern of tissue expression revealed homozygous mutations in two inbred pedigrees, including the large Bedouin kindred used to initially identify the BBS2 locus. In addition, mutations were found in three of 18 unrelated BBS probands from small nuclear families.

INTRODUCTION

Bardet–Biedl syndrome (BBS) is an autosomal recessive disorder characterized by obesity, pigmentary retinopathy, post-axial polydactyly, mental retardation and hypogonadism (1–4). A high frequency of renal abnormalities is also associated with this disorder (4). Mental retardation in BBS patients is often mild, and some patients have only learning disabilities. Onset of obesity is generally in early infancy and complications including diabetes mellitus and hypertension occur later in life. The associated retinal degeneration is usually severe and most patients become legally blind prior to 20 years of age. A relatively high incidence of BBS is found in the mixed Arab populations of Kuwait and in Bedouin tribes throughout the Middle East, most likely due to the high rate of consanguinity in these populations (5–7) and a founder effect. A relatively high frequency of BBS in Newfoundland has also been reported (4).

BBS has been shown to display a high degree of genetic heterogeneity. This was first demonstrated based on mapping studies performed in large inbred Bedouin kindreds from Israel. The high rate of consanguinity within these groups made it possible to identify inbred kindreds with multiple affected individuals that were large enough for independent linkage analysis. The first BBS locus (now referred to as BBS2) was mapped to chromosome 16 using a large inbred Bedouin kindred (8). Genetic heterogeneity was demonstrated

+To whom correspondence should be addressed. Tel: +1 319 335 6898; Fax: +1 319 335 7588; Email: val-sheffield@uiowa.edu

when a second Bedouin BBS kindred did not map to this locus. Subsequent studies in the second Bedouin kindred revealed linkage to chromosome 3 (BBS3) (9). A third Bedouin kindred showed linkage to chromosome 15 (BBS4) (10). To date, studies have demonstrated the existence of six BBS loci (8–14) and a seventh BBS locus has been postulated based on a few small BBS pedigrees that do not appear to map to any of the known loci.

Recently the first BBS gene, *MKKS*, was identified independently by two groups who hypothesized that mutations in the gene causing McKusick–Kaufman syndome (MKS) would also cause BBS (13,14). MKS is an autosomal recessive disorder characterized by post-axial polydactyly as well as genital and cardiac anomalies. Mutations in *MKKS*, a putative chaperonin gene on chromosome 20 (15), appear to account for <10% of BBS cases. The mechanism by which mutations in the *MKKS* gene cause BBS has not been determined.

Interest in the identification of genes causing BBS stems from the pleiotropic nature of the disorder and the hypothesis that identification of BBS genes will provide important insight into biochemical and developmental pathways involved in common complex disorders such as obesity and diabetes mellitus. Since the initial mapping of BBS2 to chromosome 16 in 1993, we have pursued a positional cloning approach aimed at identifying the gene causing this disorder. We now report the identification of a novel gene causing BBS2.

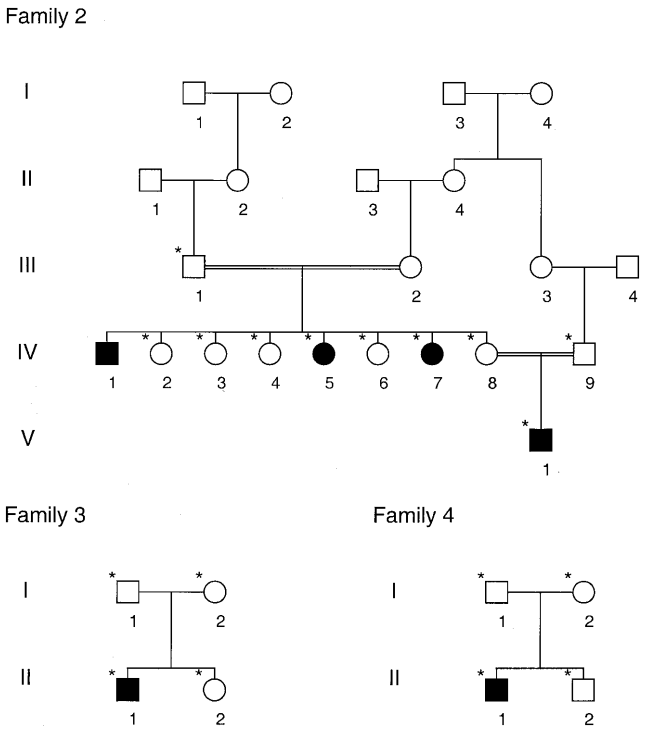

Figure 1. Pedigrees of three BBS2 families which were found to have mutations in *BBS2*. Individuals affected with BBS are indicated by filled symbols. Individuals for whom DNA was available for study are marked with an asterisk.

RESULTS

Clinical data

The clinical features of the large Bedouin kindred (Family 1) have previously been described (8). Briefly, all of the cardinal features of BBS were present in most of the affected members of this family. None of the patients had spastic paraplegia, colobomas or deafness; diagnostic features of Laurence–Moon, Biemond and Alstrom syndromes, respectively. Family 2 consisted of four affected individuals of Kurdish ancestry, all of whom had at least three of the cardinal features of BBS syndrome. Within the two families there was a clear dichotomy between affected and unaffected individuals, in that none of the unaffected individuals had any of the features of BBS. Affected individuals from both families had similar distributions of polydactyly, usually affecting both upper and lower extremities. All but one patient had polydactyly affecting at least three limbs (one individual had two-limb polydactyly). Obesity was more apparent in Family 2 compared with Family 1. Hypogenitalism was apparent in male members of both families. Two patients in Family 1 had unilateral renal hypoplasia. Retinal degeneration was present in all affected members of both families. All affected individuals in the smaller families used in this study met the diagnostic standard of having at least three of the cardinal features of BBS (3,4).

Refinement of the critical interval by genetic analysis

In 1993, linkage studies and haplotype analysis of a large inbred Bedouin kindred mapped the BBS2 locus to an 18 cM region within 16q21 flanked by the markers *D16S419* and *D16S265* (8). Analysis of additional genetic markers within this region in affected individuals narrowed the critical interval to ~6 cM. The study of unaffected individuals within the pedigree narrowed the critical interval based on the assumption of complete penetrance. One of the unaffected individuals from the large Bedouin family was found to have a recombination event at the distal end of the critical interval that narrowed the distal boundary to a region within the bacterial artificial chromosome (BAC) RP_11-152E5. Analysis of 40 additional DNA samples from unaffected family members identified an unaffected individual who had inherited the affected haplotype in the homozygous state for markers proximal to *D16S408*. This allowed the exclusion of the region proximal to *D16S408*. The refined critical interval included an ~2 cM region between the markers *D16S408* and *152e5-CA*.

A second inbred family consisting of four affected individuals was also linked to the BBS2 locus (Fig. 1, Family 2). Genotyping of DNA from three available affected individuals demonstrated that all were homozygous for the same haplotype. This haplotype was not found in the homozygous state in any of the unaffected individuals in the family. Furthermore, the affected haplotype was different to that segregating within the large inbred Bedouin family, suggesting that the mutation in each family is likely to be different. Haplotypes for key individuals from both families are shown in Figure 2.

Physical mapping

To facilitate the cloning and characterization of the *BBS2* gene, we constructed a physical map of the critical interval. An initial physical map that was based on yeast artificial chromosome (YAC) clones allowed for low-resolution localization of genetic markers and candidate genes within the critical

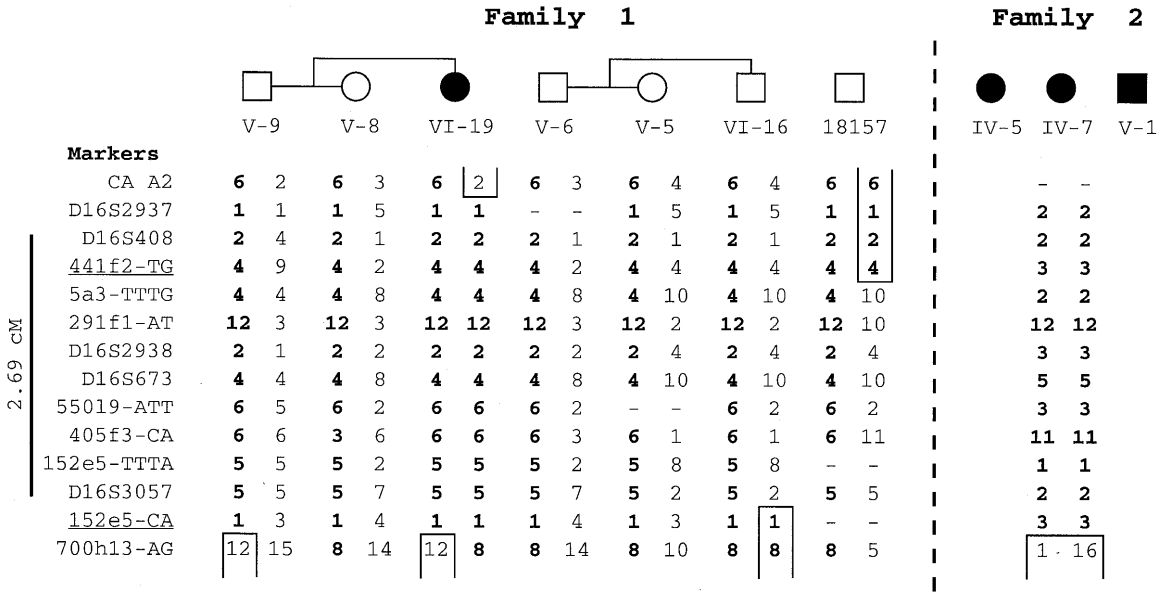

Figure 2. Haplotypes that were critical for narrowing the BBS2 critical interval are shown for individuals in families 1 and 2. The haplotypes associated with BBS are shown in bold. Affected individuals are indicated by filled symbols. Presumptive recombinant events are marked within the haplotypes. The BBS2 candidate interval is defined by the markers *441f2-TG* and *152e5-CA*, which are underlined. This represents a region of 2.69 cM.

interval. Once the genetic interval was refined to the smallest size possible, the physical map was converted to BAC clones. Radiation hybrid mapping using the Stanford G3 mapping panel was used to confirm the order obtained from the BAC-based physical maps and to anchor this region within the Stanford chromosome 16 G3 radiation hybrid map.

Candidate gene identification

The BAC-based physical map was used to select a subset of BACs for sample sequencing at 1× coverage. The sequence information obtained from sample sequencing was combined with that available from the public sequence databases and used for the identification of candidate genes for BBS2. BLASTN analysis was performed against the nr- and dbEST databases that are maintained by NCBI. This allowed us to identify a number of unique genes and Unigene EST clusters. Over 25 unique genes or EST clusters were identified, not including the multiple metallothionein genes that are known to map within the region (Fig. 3). The genes were prioritized for mutation screening based on criteria including (i) availability of known cDNA and/or genomic sequence; (ii) known expression pattern of the gene consistent with the BBS phenotype; and (iii) the availability of any functional information. Attractive candidate genes that mapped within the larger interval defined by an 'affected-only' analysis were not excluded, but were deemed to be of lower priority for analysis.

Mutation screening of candidate genes

The availability of two inbred BBS2 pedigrees that were likely to harbor independent mutations allowed us to conduct a sequencing-based mutation screen of BBS2 candidate genes. PCR amplicons that covered the coding sequence and consensus splice sites for each candidate gene were amplified from genomic DNA from an affected individual of each of the two BBS2 pedigrees and the amplification products were directly sequenced. The DNA sequences generated from the two samples were compared with each other and with sequences in GenBank. Sixteen candidate genes (Fig. 3) were screened without finding any variants that were judged to be pathological.

BBS2 gene structure and expression profile

UniGene EST cluster Hs.24809 was selected for analysis based on its broad expression pattern and on its map position within the smaller candidate interval. The UniGene cluster contained 193 ESTs and six mRNA sequences. When these sequences were assembled into contigs, two distinct, unique contigs were created. Both contigs, each representing a separate gene, mapped to BAC RP_11-5A3 within the BBS2 critical interval.

One of the contigs was found to contain an open reading frame of 1461 bp. A partial gene structure consisting of nine exons was determined. The second contig contained an open reading frame of 2163 bp (721 amino acids). The complete gene structure was ascertained for the second gene, now referred to as *BBS2* (GenBank accession no. AF342736). *BBS2* was amplified from a human fetal cDNA library and sequenced to confirm the cDNA sequence that was predicted from the EST contig. Of the 193 ESTs from UniGene cluster Hs.24809, 66 were assigned to the *BBS2* contig. Comparison of the cDNA sequence with genomic sequence revealed 17 exons (Fig. 4). The tissue distribution of these ESTs suggested that *BBS2* was widely expressed. Northern blot analysis confirmed the broad expression pattern of *BBS2* and revealed the *BBS2* mRNA to be ~3.0 kb in size (Fig. 5). This size estimate agrees with the size predicted from the genomic DNA sequence. A minor northern blot band of smaller molecular weight was apparent in tracheal tissue, suggesting possible alternative splicing or cross hybridization. Both genes were screened for mutations. While the mutation screen of the 1461 bp open reading frame of the first gene produced no evidence of

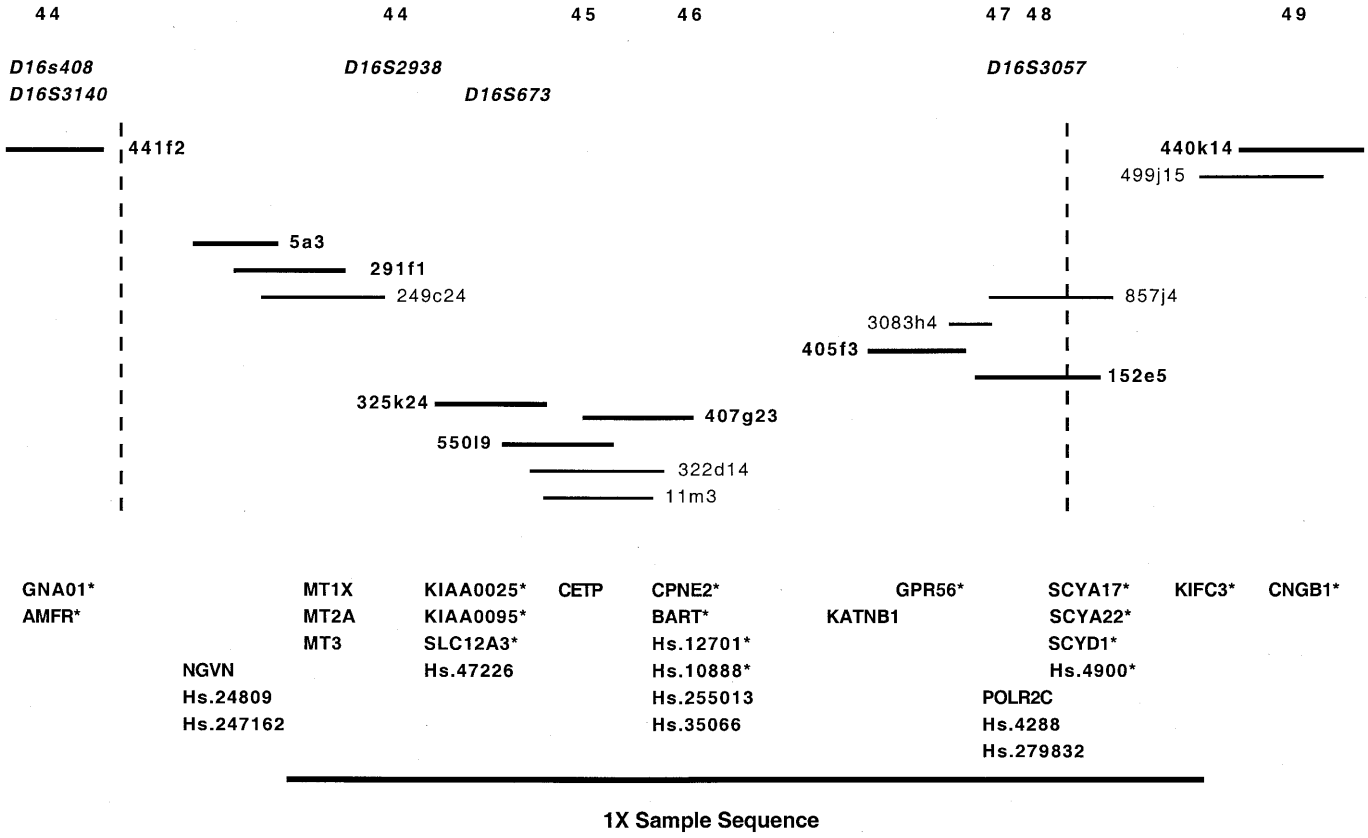

Figure 3. A physical map of the 16q21 BBS2 critical region. The numbers at the top of the figure represent radiation hybrid (RH) bin numbers according to the Stanford G3 RH map. Genetic markers in the interval are shown below the RH bin numbers. The approximate locations of BACs for which sequence was available from GenBank are also shown. Below the BACs are the known genes and UniGene EST clusters that were identified. Genes that were screened are indicated with an asterisk. Finally, the region for which 1× sample sequencing was performed is indicated.

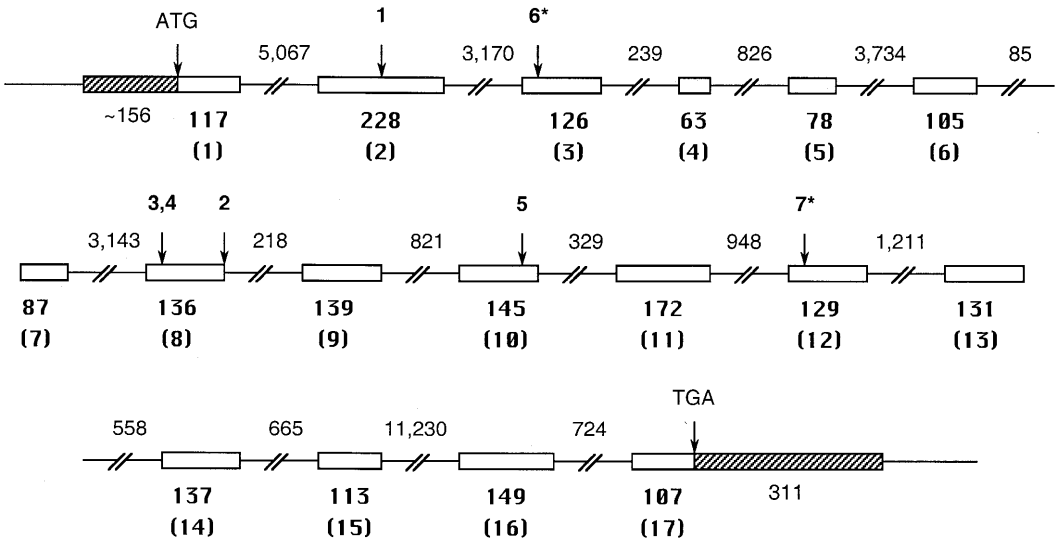

Figure 4. The gene structure for *BBS2* is shown. The exon numbers are shown in parentheses while the size of the exons in bp is shown above the corresponding exon numbers. Introns are indicated by the double hash marks with the size of each intron in bp shown above. The 5′ and 3′ UTR regions are indicated by the stippled boxes and coding regions are represented by open boxes. Numbers indicate the locations of the mutations within *BBS2* as follows: 1, T224G (Val75Gly); 2, 940delA (Frameshift); 3, C823T (Arg275Ter); 4, C814T (Arg272Ter); and 5, 1206insA (Frameshift). Two non-pathogenic variants (numbers with asterisks) were also detected: 6, A369G (Ile123Val); and 7, A1413C (Val471Val).

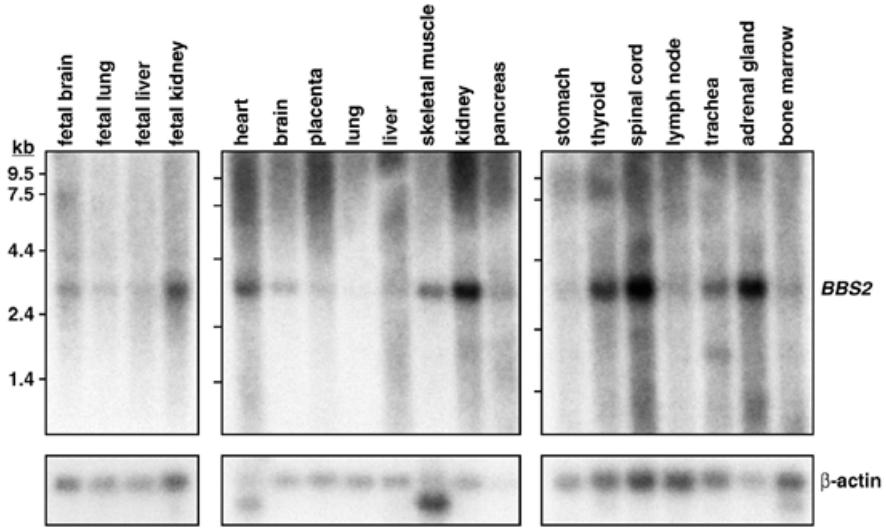

Figure 5. A northern blot analysis of *BBS2* expression in fetal and adult human tissues. Poly(A) mRNA (2 υg) isolated from human fetal and adult tissues was sequentially hybridized with ^{32}P-labeled probes for *BBS2* and *β-actin*. A 3.0 kb *BBS2* transcript is observed.

pathological variants, a number of mutations were detected in the *BBS2* gene.

BBS2 mutations

Mutation screening of *BBS2* revealed candidate mutations in both of the linked BBS2 families that were part of the initial mutation screen. Family 2 was found to harbor a homozygous 1 bp deletion in exon 8 (940delA) in all three affected individuals. This mutation predicts a protein product that is truncated 10 amino acids downstream of the 1 bp deletion at codon 324. The mutation was not found in the homozygous state in unaffected family members. The frameshift has not been detected in any other family or proband, nor in 96 control individuals.

Two sequence variants were detected on the affected chromosome in the large, inbred Bedouin BBS family. An A→G transition at nucleotide position 367 (Ile123Val) was detected in exon 3. Ile123Val is conservative and was therefore not judged to be responsible for the BBS phenotype in the family. A second variant, a T→G transversion, was found at nucleotide position 224, predicting a non-conservative valine→glycine substitution in exon 2 at residue 75 (Val75Gly). This variant is postulated to be the disease-causing mutation in this family, although we cannot exclude the possibility that both alterations may be necessary to cause the disease. Both DNA sequence variants segregate with the BBS phenotype within the family, in that all affected individuals were homozygous for both sequence variants, all obligate carriers (parents of BBS patients) were heterozygous for both variants, and no unaffected individuals were homozygous for either variant. The Val75Gly mutation was not detected in 50 unrelated Bedouin control samples.

The detection of mutations in the two BBS2 families prompted us to sequence the *BBS2* gene in 18 unrelated BBS probands from small nuclear families to identify additional mutations. One proband (Family 3) harbored an exon 8 nonsense mutation at codon 275 (Arg275Ter) in the homozygous state. His parents were found to be carriers and an unaffected sibling inherited two normal alleles. A second exon 8 homozygous nonsense mutation (Arg272Ter) was found in a second proband (Family 4). An unaffected sibling did not inherit the mutation from either parent. Finally, a homozygous 1 bp insertion (1206insA) was observed in exon 10 in a single proband (Family 5). This mutation results in a frameshift that predicts premature termination of translation five amino acids downstream from the insertion. In all, mutations were observed in two of two known BBS2 families, and in three of 18 unrelated BBS probands (Fig. 6).

Evolutionary conservation

Homology screening of the predicted BBS2 protein against the public sequence databases demonstrates that BBS2 has high similarity to genes from a number of other organisms. Sequence for the mouse ortholog for *BBS2* (GenBank accession no. AF342737) was obtained by PCR from a 17-day fetal mouse cDNA library to supplement the sequence that was available from GenBank. The mouse protein is 90% identical and 95% similar (using the BLOSUM62 similarity matrix) to the predicted human BBS2 protein. Sequences for the rat (GenBank accession no. AF342738) and zebrafish (GenBank accession no. AF342739) orthologs of *BBS2* were obtained using similar methodology. The rat ortholog was found to be 89% identical and 94% similar at the protein level and the zebrafish ortholog was found to be 74% identical and 84% similar. A comparison of the BBS2 protein sequences between human, mouse, rat and zebrafish is shown in Figure 7. A lower level of similarity was found for *Caenorhabditis elegans*, *Chlamydomonas* and *Trypanosoma* (30–46% identical; 49–57% similar).

To further investigate the disease-causing nature of the exon 2 Val75Gly variant found in Family 1, sequence was obtained from a number of organisms to determine the level of sequence conservation within this region. Valine was found at this position in human, bovine, rabbit, rat, mouse and zebrafish. In *C.elegans*, *Trypanosoma* and *Chlamydomonas*, the conservative substitution of isoleucine was found at this position. There is a high level of conservation at a number of locations within

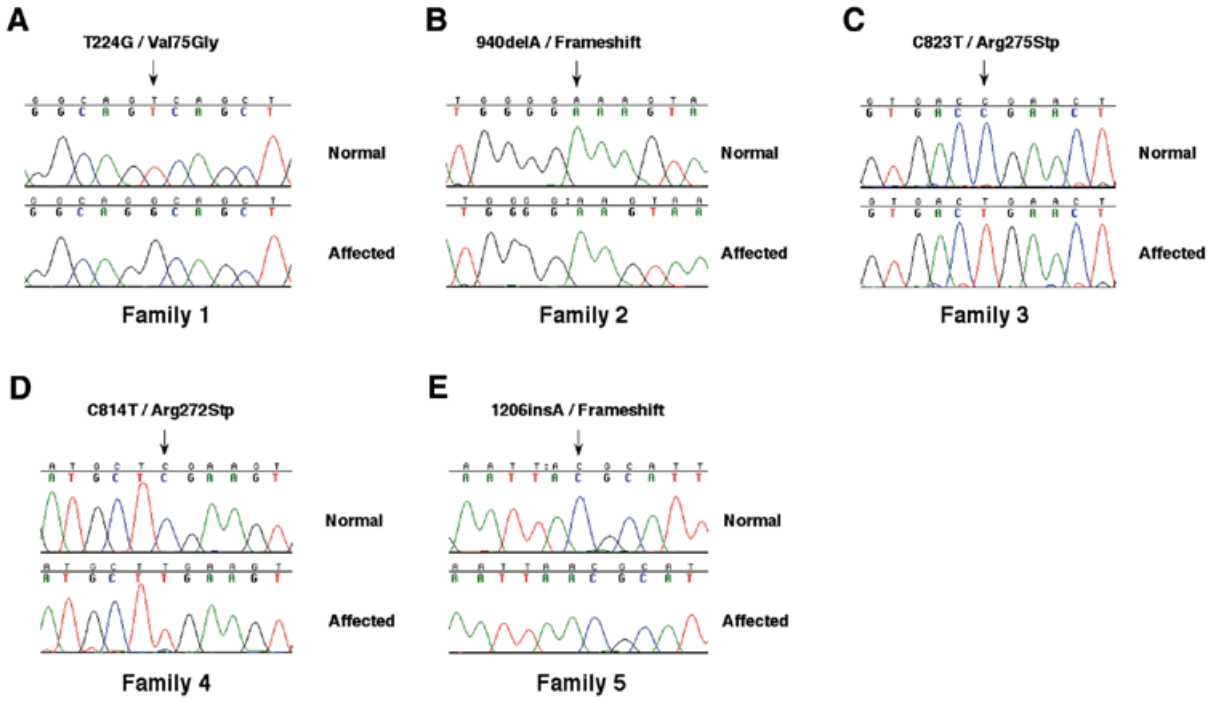

Figure 6. The five *BBS2* mutations that were detected in this study. (**A**) A T224G change (Val75Gly) was observed in a large Bedouin kindred. (**B**) A single base pair deletion (940delA) resulting in a frameshift mutation was observed in three BBS patients from a small inbred pedigree. (**C**) A C823T change (Arg275Ter) was detected in a single BBS proband. (**D**) A C814T change (Arg272Ter) was observed in a BBS proband from a small family. (**E**) A single base pair insertion (1206insA) which results in a frameshift mutation was detected in another BBS proband from a small family. All five mutations were found in the homozygous state.

this region and within the region surrounding the Ile123Val variant in exon 3. However, the isoleucine at codon 123 shows a lower level of conservation, consistent with its postulated assignment as a likely benign sequence variant.

Since the first BBS gene to be identified (*MKKS*) is a putative chaperonin, we compared *BBS2* and known chaperonin or chaperonin-like proteins. No significant similarity was found to any genes with known function by either BLAST analysis or by searching for functional domains within *BBS2*. We concluded that *BBS2* is a novel gene whose function cannot currently be determined by comparison with the primary sequence of other known genes.

DISCUSSION

In order to identify the BBS2 gene, we used genetic fine mapping to reduce the size of the BBS2 interval to ~6 cM. To further narrow the interval, we searched for unaffected individuals within the extended Bedouin kindred who had the affected haplotype on one chromosome, but were recombinant for the affected haplotype on the homologous chromosome. Two recombinant events in unaffected individuals reduced the candidate interval to ~2 cM, facilitating the construction of a BAC contig across the disease region.

The identification of the *BBS2* gene was aided by sample sequencing (~1× coverage), as well as sequence data from the public Human Genome Project, even though the complete sequence of this interval was not available. Analysis of available sequence resulted in the identification of a number of candidate genes within the narrowest interval. In order to determine which of these genes was the *BBS2* gene, we prioritized the genes for mutation screening based on a number of parameters, including sequence homology or putative functional relationship to genes in other known BBS intervals and the pattern of expression. Although this approach yielded a number of high priority candidate genes, none of these genes proved to be mutated in BBS patients. The recent identification of BBS-causing mutations in the *MKKS* gene provided initial speculation that a chaperonin gene might be found in this interval. A search of the available sequence in the interval failed to identify such a candidate gene. The eventual evaluation of the *BBS2* gene was based on the position of this gene within the narrowed disease interval and its broad pattern of expression.

Due to the genetic heterogeneity of BBS, our strategy for mutation screening of candidate genes was to focus the search for mutations by direct sequencing of DNA from an affected individual from each of two inbred families shown to link to the chromosome 16 BBS interval. One of the families was the large Bedouin kindred that allowed the initial mapping and refinement of the 16q21 interval. Focusing the primary mutation search to two inbred BBS2 families conserved resources, but ran the risk of missing the disease-causing gene by too narrowly limiting the mutation search. Nevertheless, sequencing revealed homozygous mutations in the *BBS2* gene in each of the two inbred families.

The conclusion that we have correctly identified the BBS2 gene is supported by a number of lines of evidence. First, *BBS2* maps to the narrowed disease interval and has a broad pattern of tissue expression, as would be predicted for a gene manifesting pleiotropism. *BBS2* was found to have homozygous mutations in the two inbred BBS2 pedigrees, one of which is a

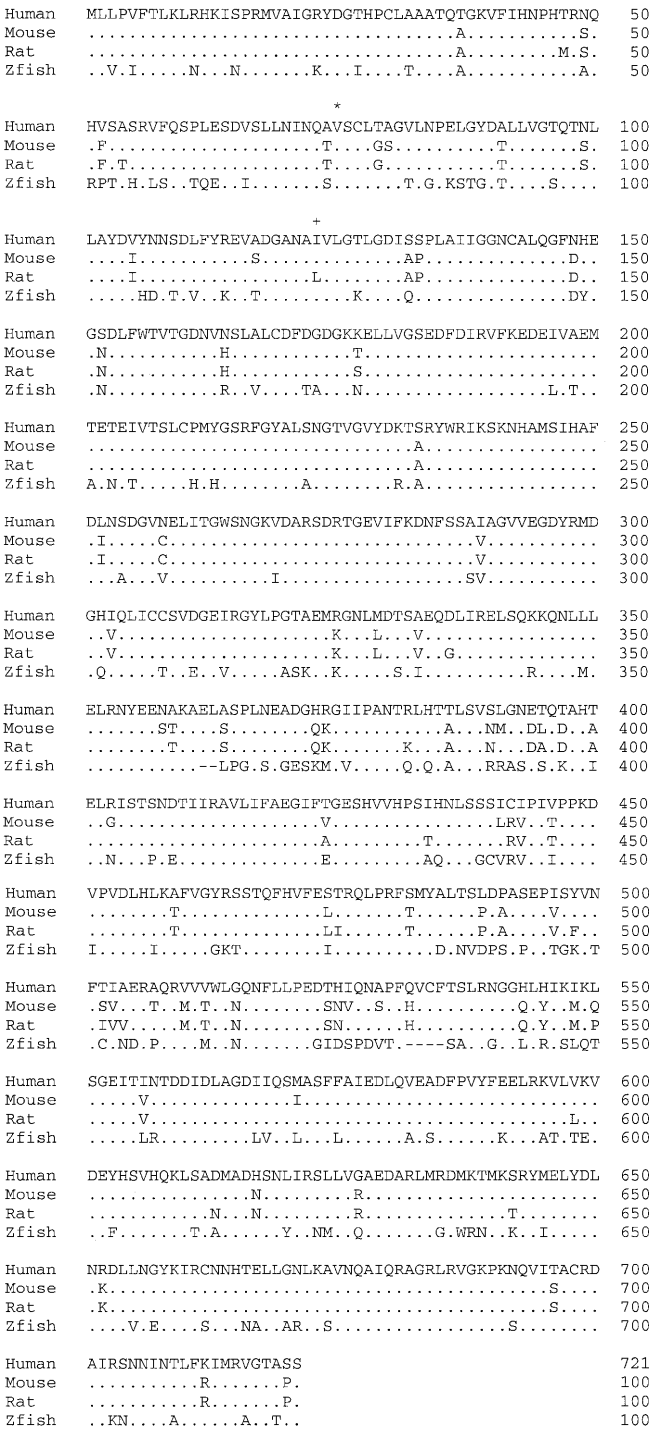

Figure 7. Comparison of the BBS2 protein sequence between human, mouse, rat and zebrafish. The human BBS2 sequence is shown on the first line of each comparison. For the other three organisms, amino acid identities are shown as dots while the actual amino acid found at a given location is shown for conservative replacements. Gaps that were introduced to align the zebrafish sequence are shown as dashes. The location of the Val75Gly mutation found in Family 1 is indicated by an asterisk and the location of the putative benign Ile123Val variant is denoted by a plus sign.

frameshift mutation. Each mutation was shown to segregate completely with the disease phenotype in the respective kindred, and neither mutation was found in 96 control individuals. In addition, *BBS2* is mutated (both nonsense and frameshift mutations) in three of 18 (17%) of BBS probands from small families, a figure that is consistent with the proportion of BBS2 cases (identified by linkage analysis) reported in the literature (16,17).

The assumption that the Val75Gly variant is the disease-causing mutation in the large Bedouin kindred is supported by the fact that the valine residue at this location is highly conserved across species. It is also the only *BBS2* sequence variant identified in this family that is not found in control samples. Of interest is the observation that the Val75Gly mutation is found in complete linkage disequilibrium with the Ile123Val variant in this population. We cannot exclude the possibility that the combination of the Val75Gly and Ile123Val variants in phase is needed for abnormal protein function.

It has been previously hypothesized that the identification of the first BBS gene would lead to the identification of other BBS genes (13,14). In the case of *MKKS*, this has not yet proven to be the case, as *BBS2* has no significant sequence similarity to *MKKS* and no currently known functional relationship. Despite this fact, we hypothesize that a functional relationship does exist. It is possible that the BBS2 protein plays an unrecognized chaperonin role or is part of a chaperonin complex. Another possibility is that the BBS2 protein is a substrate for MKKS chaperonin function. Additional experiments are needed to test these hypotheses, including the hypothesis that MKKS does indeed function as a chaperonin. Identification of *BBS2* as a BBS gene may assist in the identification of other BBS genes. In addition, studies to elucidate the function of *BBS2* are expected to help elucidate mechanisms involved in obesity, mental retardation, retinal degeneration and diabetes, as well as limb, kidney and cardiac development.

We have previously sought to characterize phenotypic differences caused by different BBS loci (BBS2, BBS3 and BBS4) based on the phenotype in three large Bedouin kindreds (18). In so doing, we had observed that the BBS2 locus was associated with less severe obesity than other BBS loci. Identification of the *BBS2* gene allows us to determine whether the relatively low body mass index in the Bedouin BBS2 kindred was due to the specific Bedouin *BBS2* allele (Val75Gly) or is characteristic of patients with mutations in *BBS2* in general. Based on the BBS2 family with the 940delA frameshift mutation (Family 2) described in this study, it appears that mutations in *BBS2* do not result in milder obesity, but rather that the specific Bedouin allele is a mild allele with respect to the obesity component of the phenotype. The fact that at least some of the phenotypic variability seen in BBS can be explained by allelic heterogeneity is supported by phenotypic differences observed between patients with MKS and BBS due to mutations in the *MKKS* gene (13–15).

MATERIALS AND METHODS

Patients and families

Signed, informed consent was obtained from each patient using protocols approved by the Institutional Review Board at the University of Iowa and collaborating institutions. Genomic DNA was isolated from whole blood according to methods that have been published previously (19).

Physical mapping reagents

YAC DNA was isolated using the DNA-Pure yeast genomic kit (CPG). BAC DNA was prepared via an alkaline lysis protocol using the Wizard Plus Miniprep kit (Promega). The precipitated DNA was washed with 70% EtOH and dried. The DNA pellet was resuspended in 50 µl of ddH_20. Plasmid DNA was prepared using a Wizard Plus Miniprep kit (Promega).

Genotyping

PCR amplification for the analysis of short tandem repeat polymorphisms (STRPs) was performed using 40 ng of genomic DNA in 8.4 µl reactions containing 1.25 µl of 10× PCR buffer [100 mM Tris–HCl pH 8.8, 500 mM KCl, 15 mM $MgCl_2$ and 0.01% gelatin (w/v)], 200 µM each of dATP, dCTP, dGTP and dTTP, 2.5 pmol of each primer and 0.2 U of Taq polymerase (Bioline). Samples were subjected to 35 cycles of 94°C for 30 s, 50, 52, 55 or 57°C as required for 30 s and 72°C for 30 s. Amplification products were electrophoresed on 6% polyacrylamide gels containing 7.7 M urea at 60 W for ~2 h. The bands were visualized by silver staining (20).

Marker typing for physical mapping was performed on 2% agarose gels using a PCR reaction size of 10 µl. Reaction conditions were as described above with the following exceptions. For markers that proved difficult to amplify using the standard Taq polymerase, we substituted an equal amount of AmpliTaq (Applied Biosystems) along with an initial incubation of the PCR mixture at 94°C for 10 min. For PCR reactions involving YAC, BAC or plasmid DNA, 1–2 ng of DNA was utilized as a template. For colony PCR, a small number of cells were inoculated into 20 υl of ddH_2O. One microliter of this suspension was used as a template for the PCR reaction.

Oligonucleotide primers for the STRPs were obtained as MapPairs (Research Genetics). The custom primers required for this study were designed using the PRIMER 0.5 program and synthesized commercially (Research Genetics or Integrated DNA Technologies).

YAC, BAC and cDNA identification

Initially, YACs were identified by searching the Whitehead Institute/MIT Genome Center database (http://www-genome.wi.mit.edu) (21) with sequence tagged sites (STSs) known to be in the 16q21 region. Subsequently YACs and BACs were identified by a PCR-based screening assay of pooled libraries (Research Genetics or Genome Systems) using various STSs within each region. ESTs were identified by a BLASTN (22) search of the public dbEST database available through a web interface at NCBI.

Gene identification and characterization

Raw SCF files from ABI 377 sequencers were imported directly into the Sequencher version 3.1 program (Gene-Codes). Contigs were generated by comparing all fragments in a project with the parameters of a ≥50 bp overlap in sequence with 80% level of homology. Genomic sequence of BACs from the 16q21 region was submitted to the BLAST server at NCBI for a BLASTN (22) analysis on both the nr and dbEST databases. Any region which gave a significant score ($P < 10^{-5}$) was also submitted for a BLASTX screen of the SWISS-PROT database. EST sequence was obtained from GenBank and SCF files from the WashU-Merck ftp site (ftp://genome.wustl.edu).

Table 1. *BBS2* gene structure and PCR primers for mutation screening

Exon	Size (bp)	Splice acceptor	Splice donor	Forward primer (5′→3′)	Reverse primer (5′→3′)
1	117	–	GCAAGgtaac	GCGTGAGGCCAGCTCCGCTGC	GCGCGGCCGGCGGAGATCCTG
2	208	ttcagGTTTT	GAGAGgcaag	TTTTAAGGGAATGTAATTAGT	TGGACATTAATGAGTAATGAC
3	126	cttagGTAGC	GGACGgtatg	TTTACTCAAAATCTGCTCAGT	AATATTATTACTCAGTAGAGT
4	63	ttcagGTTAC	AAGAGgtatg	AATCCTCTCCTTCATGTAGCT	GGAGAAGCTTACACTTCTGTC
5	78	ttcagCTTCT	CAGAGgtaag	AGAAGCAGCATGCAAAGTACT	TCATCTGACAGTACTGATCTA
6	105	tgcagATAGT	TTAAAgttag	TATAAAGCCGTACTTGACAGT	CAATAACTATCAAGCGCCTGA
7	87	ttcagTCGAA	GGAAGgtaag	TATTGTGAGACTTCTGTGCTA	TGTTACTGTTCTAAGTCCTAC
8	136	tgtagGTTGA	GGAAAgtaaa	AGAATACTCTTGAAAACTGCT	ATCTCGGTACAAATACTTCAG
9	139	ttcagTCCGG	CCAAGgtagg	TAAGAGCAGGTAATTGATGAC	CCCTGGCAATGACACTCTCAT
10	145	tgcagGCTGA	TAATGgtaag	GGCTCTGTCTTTTGAAGCTGA	CCAAGACAGAGGAAGACTCTG
11	172	tgcagACACC	AGCAGgtgac	ACCTCCTGACCTCGTGATCTG	CCCCAAGAATCCACTGGGCAT
12	129	catagCACCC	AGAGGgtgag	CCTTAAATATCAATTGATGAC	ACTGCTACCAATATAACACAT
13	131	tcaagGTTGT	GAGAGgtaat	GAATGTTACTTAAGAGCATAG	CTGAATGGTAAACACCACATG
14	137	ggtagATCAC	TTAAGgtgag	GCTAAGTTTGTCTAACATCTG	ACATAAGTACATTTGTAGTAC
15	113	tccagGTGGA	GACATgtgag	TTAATTGGTATAAGCGAACAG	TTATACTTCTATTGGTAACAT
16	149	cacagGAAAA	GCGGGgtaag	TAAGCTTGCCATATCAACATG	ATATGAATTATTGGATGCTAC
17	107	tgcagTTGGA	–	TTGTTTTAAAACTGACGTCTA	ATTCAGCAACAGTACTACTAC

Sequencing

PCR products for sequencing were amplified in a 50 µl reaction size and purified using the Qiaquick PCR Clean-up kit (Qiagen). Plasmid DNA (150 ng in 4.5 µl) or 4.5 µl of purified PCR product was used as a template for sequencing reactions. One microliter of primer (20 pmoles) and 4.5 µl of terminator sequencing mix (Amersham Pharmacia Biotech and Applied Biosystems) were added for a final reaction volume of 10 µl. Cycling conditions were performed as specified by the manufacturer. The sequencing reactions were precipitated in the presence of linear acrylamide and resuspended in 2 µl of loading buffer. The reactions were analyzed on an ABI 377 using a run time of 3 h.

Mutation detection and confirmation

Mutation detection was performed by direct sequencing of PCR amplification products. The primers used to amplify the *BBS2* gene are shown in Table 1. Control samples were assayed by single strand conformation polymorphism (SSCP) analysis. For SSCP, PCR products were electrophoresed on SSCP gels (5 ml of glycerol, 5 ml of 5× TBE, 12.5 ml of 37.5:1 acrylamide/bis and 77.5 ml of ddH_2O) for 3–4 h in 0.25× TBE at room temperature. Gels were silver stained as described above. Abnormal variants were sequenced and compared with a control sample to detect any changes from that of the normal sequence.

Northern blot analysis

Human multiple tissue northern (MTN) blots I and III and human fetal MTN blot II were obtained from Clontech. The blots were hybridized with a 300 bp DNA probe derived from the 3′ untranslated region (UTR) of the human *BBS2* gene. The probe was amplified by PCR using the BBS2-forward (5′-AATAACCTTGGTGAGTTGTAC-3′) and BBS2-reverse (5′-ATACAAATGGGCAATTCTGAT-3′) primers. The probe was labeled with ^{32}P-dCTP using Ready-To-Go DNA labeling beads (Amersham Pharmacia Biotech). Hybridization and autoradiography were performed as described previously (23). The blots were stripped of radioactivity and re-hybridized with a cDNA probe for β-actin (Clontech) to assess equal loading of the RNA.

ACKNOWLEDGEMENTS

We are grateful to the patients and their families for their participation in this study. We also thank Michael Andrews, Gretel Beck and Christine Hartzler for technical assistance, Terry Braun, Kirk Mykytyn and Mythrei Shastri for helpful discussions and Denise Crouch for administrative assistance. This work was supported by the following grants and organizations: NIH grant R01-EY-11298 (E.M.S. and V.C.S.), Foundation Fighting Blindness (S.G.J., E.M.S. and V.C.S.), Carver Endowment for Molecular Ophthalmology (E.M.S. and V.C.S.) and Research to Prevent Blindness, New York, NY (unrestricted grant to the Department of Ophthalmology, University of Tennesse, Memphis). V.C.S. is an Associate Investigator for the Howard Hughes Medical Institute.

REFERENCES

1. Bardet, G. (1920) Sur un syndrome d'obesite infantile avec polydactylie et retinite pigmentaire (contribution a l'etude des formes cliniques de l'obesite hypophysaire). PhD Thesis, Paris, France.

2. Biedl, A. (1922) Ein Geschwisterpaar mit adipose-genitaler Dystrophie. *Dtsch. Med. Woschenschr.*, **48**, 1630.
3. Schachat, A.P. and Maumenee, I.H. (1982) Bardet-Biedl syndrome and related disorders. *Arch. Ophthalmol.*, **100**, 285–288.
4. Green, J.S., Parfrey, P.S., Harnett, J.D., Farid, N.R., Cramer, B.C., Johnson, G., Heath, O., McManamon, P.J., O'Leary, E. and Pryse-Phillips, W. (1989) The cardinal manifestations of Bardet-Biedl syndrome, a form of Laurence-Moon-Biedl syndrome. *New Engl. J. Med.*, **321**, 1002–1009.
5. Farag, T.I. and Teebi, A.S. (1988) Bardet-Biedl and Laurence-Moon syndromes in a mixed Arab population. *Clin. Genet.*, **33**, 78–82.
6. Farag, T.I. and Teebi, A.S. (1989) High incidence of Bardet-Biedl syndrome among the Bedouin [letter]. *Clin. Genet.*, **36**, 463–464.
7. Teebi, A.S. (1994) Autosomal recessive disorders among Arabs: an overview from Kuwait. *J. Med. Genet.*, **31**, 224–233.
8. Kwitek-Black, A.E., Carmi, R., Duyk, G.M., Buetow, K.H., Elbedour, K., Parvari, R., Yandava, C.N., Stone, E.M. and Sheffield, V.C. (1993) Linkage of Bardet-Biedl syndrome to chromosome 16q and evidence for nonallelic genetic heterogeneity. *Nature Genet.*, **5**, 392–396.
9. Sheffield, V.C., Carmi, R., Kwitek-Black, A., Rokhlina, T., Nishimura, D., Duyk, G.M., Elbedour, K., Sunden, S.L. and Stone, E.M. (1994) Identification of a Bardet-Biedl syndrome locus on chromosome 3 and evaluation of an efficient approach to homozygosity mapping. *Hum. Mol. Genet.*, **3**, 1331–1335.
10. Carmi, R., Rokhlina, T., Kwitek-Black, A.E., Elbedour, K., Nishimura, D., Stone, E.M. and Sheffield, V.C. (1995) Use of a DNA pooling strategy to identify a human obesity syndrome locus on chromosome 15. *Hum. Mol. Genet.*, **4**, 9–13.
11. Leppert, M., Baird, L., Anderson, K.L., Otterud, B., Lupski, J.R. and Lewis, R.A. (1994) Bardet-Biedl syndrome is linked to DNA markers on chromosome 11q and is genetically heterogeneous. *Nature Genet.*, **7**, 108–112.
12. Young, T.L., Penney, L., Woods, M.O., Parfrey, P.S., Green, J.S., Hefferton, D. and Davidson, W.S. (1999) A fifth locus for Bardet-Biedl syndrome maps to chromosome 2q31. *Am. J. Hum. Genet.*, **64**, 900–904.
13. Katsanis, N., Beales, P.L., Woods, M.O., Lewis, R.A., Green, J.S., Parfrey, P.S., Ansley, S.J., Davidson, W.S. and Lupski, J.R. (2000) Mutations in MKKS cause obesity, retinal dystrophy and renal malformations associated with Bardet-Biedl syndrome. *Nature Genet.*, **26**, 67–70.
14. Slavotinek, A.M., Stone, E.M., Mykytyn, K., Heckenlively, J.R., Green, J.S., Heon, E., Musarella, M.A., Parfrey, P.S., Sheffield, V.C. and Biesecker, L.G. (2000) Mutations in MKKS cause Bardet-Biedl syndrome. *Nature Genet.*, **26**, 15–16.
15. Stone, D.L., Slavotinek, A., Bouffard, G.G., Banerjee-Basu, S., Baxevanis, A.D., Barr, M. and Biesecker, L.G. (2000) Mutation of a gene encoding a putative chaperonin causes McKusick-Kaufman syndrome. *Nature Genet.*, **25**, 79–82.
16. Bruford, E.A., Riise, R., Teague, P.W., Porter, K., Thomson, K.L., Moore, A.T., Jay, M., Warburg, M., Schinzel, A., Tommerup, N. *et al.* (1997) Linkage mapping in 29 Bardet-Biedl syndrome families confirms loci in chromosomal regions 11q13, 15q22.3-q23, and 16q21. *Genomics*, **41**, 93–99.
17. Woods, M.O., Young, T.L., Parfrey, P.S., Hefferton, D., Green, J.S. and Davidson, W.S. (1999) Genetic heterogeneity of Bardet-Biedl syndrome in a distinct Canadian population: evidence for a fifth locus. *Genomics*, **55**, 2–9.
18. Carmi, R., Elbedour, K., Stone, E.M. and Sheffield, V.C. (1995) Phenotypic differences among patients with Bardet-Biedl syndrome linked to three different chromosome loci. *Am. J. Med. Genet.*, **59**, 199–203.
19. Nishimura, D.Y., Swiderski, R.E., Alward, W.L., Searby, C.C., Patil, S.R., Bennet, S.R., Kanis, A.B., Gastier, J.M., Stone, E.M. and Sheffield, V.C. (1998) The forkhead transcription factor gene FKHL7 is responsible for glaucoma phenotypes which map to 6p25. *Nature Genet.*, **19**, 140–147.
20. Bassam, B.J., Caetano-Anolles, G. and Gresshoff, P.M. (1991) Fast and sensitive silver staining of DNA in polyacrylamide gels. *Anal. Biochem.*, **196**, 80–83.
21. Hudson, T.J., Stein, L.D., Gerety, S.S., Ma, J., Castle, A.B., Silva, J., Slonim, D.K., Baptista, R., Kruglyak, L., Xu, S.H. *et al.* (1995) An STS-based map of the human genome. *Science*, **270**, 1945–1954.
22. Altschul, S.F., Gish, W., Miller, W., Myers, E.W. and Lipman, D.J. (1990) Basic local alignment search tool. *J. Mol. Biol.*, **215**, 403–410.
23. Swiderski, R.E., Ying, L., Cassell, M.D., Alward, W.L., Stone, E.M. and Sheffield, V.C. (1999) Expression pattern and *in situ* localization of the mouse homolog of the human MYOC (GLC1A) gene in adult brain. *Brain Res. Mol. Brain Res.*, **68**, 64–72.